

Classical and Quantum-Mechanical Turbulence in He II Heat Flow*

J. T. TOUGH

Ohio State University, Columbus, Ohio

(Received 12 November 1965)

The theory of the He II thermal counterflow process in wide ($d > 10^{-3}$ cm) channels is investigated on the assumption that both the normal and superfluid components make a transition from a laminar to a turbulent type of flow. A critical heat current W_0 is identified with the superfluid transition. The superfluid turbulent state is taken to be essentially that described by Vinen in terms of quantized vortex line and has an associated mutual friction. A second critical heat current W_c is identified with the normal-fluid transition. It is argued that this transition is essentially of a classical turbulent type, with the added condition that the critical value of the Reynolds number must depend on the extent of mutual-friction coupling. This interpretation is shown to be consistent with experimentally observed critical heat currents, as well as with critical-velocity effects found in other types of flow. The assumption of two critical heat currents defines three distinct flow regions. It is shown that these three regions are essentially the same as those found experimentally by Allen, Griffiths, and Osborne. On the basis of some simplifying assumptions regarding the normal-fluid turbulent state, the temperature and pressure gradients accompanying thermal counterflow are calculated. Comparison with experiment shows good qualitative and often quantitative agreement. It is also shown that the model developed can be successfully used to interpret experiments involving flows of a nonthermal counterflow type.

INTRODUCTION

EARLY experiments on the heat transfer in He II revealed an anomalously high thermal conductivity for sufficiently small heat flow. This is now understood in terms of a two-fluid model in which heat is transferred by the flow of a viscous normal fluid accompanied by a counterflow of an inviscid superfluid. Hydrodynamic equations have been developed for these two fluids, and are consistent with experimental observation for low heat flow.

In heat currents greater than some critical value, nonlinear effects are observed. Vinen¹ has shown that for heat currents not too near the critical value, many experimental results are consistent with a model of superfluid turbulence involving quantized vortex lines. Some more recent measurements, however, are more readily understood in terms of a turbulent normal fluid.²⁻⁵ The purpose of this paper is to show that a model based on turbulence in both the normal and superfluid components offers a qualitative and often quantitative agreement with experiment. Not only does the model offer explanations for several heretofore unexplained effects, but exhibits in several instances the similarity between heat conduction and rotation effects.

The discussion will generally be restricted to temperature and pressure gradients accompanying thermal counterflow in wide ($d > 10^{-3}$ cm) channels, although other systems will be considered when there appears to be some unifying feature. Subcritical heat currents

are considered in Sec. I in order to present the linearized two-fluid equations. In Sec. II the critical heat currents corresponding to the two turbulent flows are considered in detail. In particular, the effect of mutual friction on the normal-fluid transition is shown to be consistent with experimentally observed critical heat currents. In Sec. III the effects of turbulence in the two fluids is considered. The temperature and pressure gradients arising from normal fluid and superfluid turbulence are compared with experiment in Sec. IV.

I. SUBCRITICAL HEAT CURRENTS

There are several developments of the two-fluid hydrodynamic equations.^{6,7} The generally accepted form is

$$\rho_n \partial \mathbf{v}_n / \partial t + \rho_n (\mathbf{v}_n \cdot \nabla) \mathbf{v}_n = \eta_n \nabla^2 \mathbf{v}_n - (\rho_n / \rho) \nabla P - \rho_s S \nabla T + \mathbf{F}_{sn}, \quad (1)$$

$$\rho_s \partial \mathbf{v}_s / \partial t + \rho_s (\mathbf{v}_s \cdot \nabla) \mathbf{v}_s = (-\rho_s / \rho) \nabla P + \rho_s S \nabla T - \mathbf{F}_{sn}, \quad (2)$$

where ρ_n and ρ_s are the normal and superfluid densities, ρ is the total fluid density ($\rho = \rho_n + \rho_s$), \mathbf{v}_n and \mathbf{v}_s are the normal and superfluid velocities, η_n the normal fluid viscosity, ∇P and ∇T the pressure and temperature gradients, S the entropy per gram, and \mathbf{F}_{sn} the mutual friction force. If we consider only subcritical heat currents, $\mathbf{F}_{sn} = 0$, and we can assume the velocities \mathbf{v}_n and \mathbf{v}_s are small and time-independent. Thus we have

$$\nabla P = \rho S \nabla T \quad (3)$$

London's equation, and

$$(-\rho_n / \rho) \nabla P = \rho_s S \nabla T - \eta_n \nabla^2 \mathbf{v}_n. \quad (4)$$

* This work was supported in part by the National Science Foundation.

¹ W. F. Vinen, Proc. Roy. Soc. (London) **A240**, 114 (1957); **A240**, 128 (1957); **A242**, 493 (1957); **A243**, 400 (1957).

² C. E. Chase, Phys. Rev. **127**, 361 (1962); **131**, 1898 (1963).

³ F. A. Staas, K. W. Taconis, and W. M. van Alphen, Physica **27**, 893 (1961).

⁴ J. T. Tough, W. D. McCormick, and J. G. Dash, Phys. Rev. **140**, A1524 (1965).

⁵ J. F. Allen, D. J. Griffiths, and D. V. Osborne, Proc. Roy. Soc. (London) **A287**, 328 (1965).

⁶ L. D. Landau and E. M. Lifshitz, *Fluid Mechanics* (Addison-Wesley Publishing Company, Inc., Reading, Massachusetts, 1959).

⁷ J. G. Daunt and R. S. Smith, Rev. Mod. Phys. **26**, 172 (1954).

Combining Eqs. (3) and (4) gives

$$\nabla P = \eta_n \nabla^2 \mathbf{v}_n \quad (5)$$

an equation equivalent to the Poiseuille equation in classical hydrodynamics. In the case of flow through a circular tube of radius a under a constant pressure gradient, this equation can be solved to give⁶

$$\langle \mathbf{v}_n \rangle = -(a^2/8\eta_n) \nabla P, \quad (6)$$

where $\langle \mathbf{v}_n \rangle$ is the average of \mathbf{v}_n over the tube cross section.

In terms of the two-fluid model, the normal fluid carries the total entropy of the fluid, and a heat current \mathbf{W} (erg/cm² sec) is supported by a flow of the normal fluid at $\langle \mathbf{v}_n \rangle$:

$$\mathbf{W} = \rho ST \langle \mathbf{v}_n \rangle. \quad (7)$$

If we also impose a condition of no net mass transfer, we have

$$\rho_n \mathbf{v}_n + \rho_s \mathbf{v}_s = 0. \quad (8)$$

For subcritical heat currents, we then have from Eqs. (6) and (7):

$$\nabla P = -8\eta_n W / a^2 \rho ST. \quad (9)$$

Combining this with Eq. (3) gives

$$\nabla T = -8\eta_n W / a^2 (\rho ST)^2. \quad (10)$$

Equations (9) and (10) have been used to compute η_n from measurements of ∇P or ∇T in thermal counterflow. The viscosity measured by this technique is found to agree closely with that found by most other methods, with the exception of the oscillating disc.⁸ The experimental evidence, therefore, seems to verify the substantial validity of Eqs. (9) and (10).

II. THE CRITICAL HEAT CURRENTS

In a series of theoretical and experimental papers,¹ Vinen has given a detailed theory of superfluid turbulence. In Vinen's model, the turbulent superfluid is pictured as containing a "tangled mass of quantized vortex lines." The superfluid velocity necessary for the production of a single vortex line at $T=0$ in a tube of diameter " d " has been given by Feynman⁹ as

$$v_s = (\hbar/md) \ln(d/2a_0), \quad (11)$$

where a_0 is the vortex core radius. More detailed derivations have been given,¹⁰⁻¹² but most result in an expression in order of magnitude agreement with

$$v_s d \approx \hbar/m. \quad (12)$$

⁸ D. F. Brewer and D. O. Edwards, Proc. Roy. Soc. (London) **A251**, 247 (1959).

⁹ R. P. Feynman, *Progress in Low Temperature Physics*, edited by C. J. Gorter (North-Holland Publishing Company, Amsterdam, 1955), Vol. 1, Chap. II.

¹⁰ V. P. Peshkov, in *Proceedings of the VIIth International Conference on Low Temperature Physics* (University of Toronto Press, Toronto, 1961), p. 555.

¹¹ J. C. Fineman and C. E. Chase, Phys. Rev. **124**, 1 (1963).

¹² A. C. Fetter, Phys. Rev. Letters **10**, 507 (1963).

We shall denote by v_{s0} this critical value of the superfluid velocity. The corresponding heat current W_0 is then

$$W_0 = (\rho_s/\rho_n) \rho ST v_{s0} \quad (13)$$

from Eqs. (7) and (8). The presence of vortex lines in the superfluid provides scattering centers for the excitations composing the normal fluid.^{13,14} This scattering results in an effective mutual friction between the two fluids, represented in Eqs. (1) and (2) by \mathbf{F}_{sn} . By considering the processes by which vortex line is generated and decays, Vinen is able to show that \mathbf{F}_{sn} is approximately of the form

$$\mathbf{F}_{sn} = A \rho_s \rho_n |\mathbf{v}|^2 \mathbf{v}, \quad (14)$$

where \mathbf{v} is the relative velocity $\mathbf{v} = \mathbf{v}_s - \mathbf{v}_n$. Vinen's derivation assumes $v_s \gg v_{s0}$ (so that the distribution of line may be assumed random) and is thus not inconsistent with the form

$$\mathbf{F}_{sn} = A \rho_s \rho_n |\mathbf{v} - \mathbf{v}_0|^2 \mathbf{v}; \quad \mathbf{v} \geq \mathbf{v}_0 \quad (15)$$

which more closely fits the experimental data. By considering the process of vortex annihilation at the channel walls, Vinen has also shown that a mutual friction similar to that described by Eq. (15) would arise. In this expression for \mathbf{F}_{sn} we mean by \mathbf{v}_0 the value of $\mathbf{v} = \mathbf{v}_s - \mathbf{v}_n$ when $v_s = v_{s0}$ or $W = W_0$. Equation (15) then assures that no mutual friction appears until vortex lines are formed in the superfluid. The quantity A in Eq. (15) is calculated by Vinen, but is generally taken as an experimental parameter.¹⁵ It is clear physically that there must be an initial "build-up" process during which a "tangled mass of vortex line" is formed, and \mathbf{F}_{sn} approaches its equilibrium value in Eq. (15). For simplicity we shall assume that Eq. (15) is valid for all $v_s > v_{s0}$ and defer further discussion of the "build-up" process to Sec. IV.

The onset of superfluid turbulence at W_0 provides one mechanism for nonlinear hydrodynamic behavior. We shall assume that there is also a transition to turbulent flow in the normal fluid at a heat current W_c , where

$$W_c = \rho ST v_{nc} \quad (16)$$

and v_{nc} is the critical normal-fluid velocity.

If we were to assume there was no interaction between the normal fluid and superfluid (that is, if $\mathbf{F}_{sn} = 0$) then we would expect from Eq. (1) that v_{nc} would be given by a constant value of the Reynolds number,

$$R_n = \rho_n v_{nc} d / \eta_n \quad (17)$$

consistent with the channel geometry of characteristic dimension d . For a critical value of R_n of about 2×10^3 (typical for tubes of circular cross section), Eq. (17)

¹³ G. W. Rayfield and F. Reif, Phys. Rev. **136**, A1194 (1964).

¹⁴ H. E. Hall and W. F. Vinen, Proc. Roy. Soc. (London) **A238**, 204 (1956); **A238**, 215 (1956).

¹⁵ H. C. Kramers, Physica **26**, 581 (1960).

gives very large values of v_{nc} . For temperatures larger than about 1.0°K, the corresponding value of v_s ($v_s = v_{nc}\rho_n/\rho_s$) is many times larger than the critical value v_{s0} given by Eq. (11). In this case the superfluid would be turbulent and $F_{sn} \neq 0$, so that the assumption of no interaction between fluids is no longer valid.

We must therefore consider the transition to turbulent flow of the normal fluid coupled to the superfluid by mutual friction. We adopt the technique of Chandrasekhar and Donnelly¹⁶ which has proved successful in He II rotation analysis. These authors adapt the perturbation stability method of classical hydrodynamics^{6,17} to the two-fluid system. In order to illustrate the classical method, we briefly consider a fluid described by the Navier-Stokes equation:

$$\rho D\mathbf{v}/Dt = -\nabla p + \eta \nabla^2 \mathbf{v}, \quad (18)$$

where

$$D\mathbf{v}/Dt = \partial\mathbf{v}/\partial t + (\mathbf{v} \cdot \nabla)\mathbf{v}. \quad (19)$$

One assumes that the transition to turbulent flow is characterized by the appearance of small, time-dependent velocity fields superimposed on the laminar flow. We thus wish to consider the stability of a perturbation $\mathbf{v}'(\mathbf{r}, t)$ where

$$\mathbf{v} = \mathbf{V}(\mathbf{r}) + \mathbf{v}'(\mathbf{r}, t) \quad (20)$$

and

$$\nabla p = \nabla P + \nabla p'. \quad (21)$$

Here $\mathbf{V}(\mathbf{r})$ and ∇P are the velocity and pressure gradient in laminar flow. Assuming that the fluid is incompressible, we also have the continuity equation

$$\nabla \cdot \mathbf{v} = 0. \quad (22)$$

Substituting Eqs. (20) and (21) into Eq. (18) gives to first order in \mathbf{v}' :

$$\rho \partial \mathbf{v}' / \partial t + \rho (\mathbf{V} \cdot \nabla) \mathbf{v}' + \rho (\mathbf{v}' \cdot \nabla) \mathbf{V} = \eta \nabla^2 \mathbf{v}' - \nabla p', \quad (23)$$

where we have used

$$\eta \nabla^2 \mathbf{V} - \nabla P = 0 \quad (24)$$

for the laminar values. Equation (23) is a linear differential equation with constant coefficients and thus has solutions of the form

$$\mathbf{v}'(\mathbf{r}, t) = \mathbf{f}(\mathbf{r}) \exp i(\mathbf{k} \cdot \mathbf{r} - \omega t), \quad (25)$$

where ω is in general complex. Substitution of Eq. (25) into Eq. (23) then leads to an algebraic equation for $\omega(k, R)$, where

$$R = \rho \bar{v} d / \eta \quad (26)$$

is the Reynolds number and d is a characteristic dimension of the system. The critical Reynolds number is

¹⁶ S. Chandrasekhar and R. J. Donnelly, Proc. Roy. Soc. (London) A241, 9 (1957).

¹⁷ C. C. Lin, *The Theory of Hydrodynamic Stability* (Cambridge University Press, London, 1955).

thus the minimum value of R such that

$$\text{Im} \omega(k, R) > 0. \quad (27)$$

For $R > R_c$, then, the perturbation \mathbf{v}' will increase in time. At large values of R these perturbations occur over a wide range of (real) frequencies and wave numbers, and the flow is fully turbulent.

Chandrasekhar and Donnelly¹⁶ have used this technique to examine the stability of He II flow between rotating cylinders, explicitly introducing a mutual friction coupling force in the two-fluid equations. They find that there are two critical velocities corresponding to the superfluid and normal fluid, respectively. The superfluid instability is of the classical Rayleigh type for inviscid fluids, and the normal-fluid instability is of the classical Taylor type for viscous fluids. In the limit of zero mutual friction coupling, these critical velocities reduce to their classical values. For nonzero coupling, however, the effect of the mutual friction is to modify the stability. That is, in the case of the normal fluid, the critical Taylor number (analogous to the critical Reynolds number in parallel flow) becomes a function of the coupling strength

$$C = Bd^2/\omega\nu, \quad (28)$$

where B is the mutual friction constant for rotation,¹⁴ d is the width of the angular gap, ω is the rotation frequency and $\nu = \eta_n/\rho_n$. Preliminary experimental results are in complete agreement with these calculations.¹⁸

In the case of He II thermal counterflow the situation is somewhat different. Here we assume the mutual friction is set up by the transition of the superfluid to turbulent flow. Thus, only the normal fluid transition can be affected by the mutual friction. We thus anticipate, in analogy to the rotation situation, that the critical Reynolds number appropriate to the onset of normal fluid turbulence will be a function of the mutual friction coupling.

We shall not attempt a perturbation stability calculation of the coupled two-fluid equations for thermal counterflow. Indeed, the calculation of the simple Navier-Stokes equation for parallel flow is quite formidable.¹⁷ Rather, we shall set up the equations and show how they can be used to interpret experimental data. We take for the coupled two-fluid equations (see Eqs. 1 and 2):

$$\rho_n D\mathbf{v}_n/Dt = \eta_n \nabla^2 \mathbf{v}_n - \nabla p_n + \mathbf{F}_{sn}, \quad (29)$$

$$\rho_s D\mathbf{v}_s/Dt = -\nabla p_s - \mathbf{F}_{sn}, \quad (30)$$

where we take \mathbf{F}_{sn} in the simplified form

$$\mathbf{F}_{sn} = A \rho_s \rho_n |\mathbf{v}|^2 \mathbf{v} \quad (31)$$

and define

$$\nabla p_n = (\rho_n/\rho) \nabla p + \rho_s S \nabla T, \quad (32)$$

$$\nabla p_s = (\rho_s/\rho) \nabla p - \rho_s S \nabla T, \quad (33)$$

¹⁸ R. J. Donnelly, Phys. Rev. Letters 3, 507 (1959).

such that

$$\nabla p = \nabla p_n + \nabla p_s. \quad (34)$$

Addition of Eqs. (30) and (31) gives another fundamental equation

$$\rho_n D\mathbf{v}_n/Dt + \rho_s D\mathbf{v}_s/Dt = \eta_n \nabla^2 \mathbf{v}_n - \nabla p. \quad (35)$$

Introducing the perturbation as in Eqs. (20) and (21),

$$\mathbf{v}_n = \mathbf{V}_n + \mathbf{v}_n'; \quad \nabla p_n = \nabla P_n + \nabla p_n' \quad (36)$$

$$\mathbf{v}_s = \mathbf{V}_s + \mathbf{v}_s'; \quad \nabla p_s = \nabla P_s + \nabla p_s' \quad (37)$$

$$\mathbf{v} = (\mathbf{V}_s - \mathbf{V}_n) + (\mathbf{v}_s' - \mathbf{v}_n') = \mathbf{V} + \mathbf{v}';$$

$$\nabla p = \nabla P + \nabla p'. \quad (38)$$

Using these expressions in Eqs. (30) and (35) gives to first order in the perturbations:

$$\rho_s \partial \mathbf{v}_s' / \partial t + \rho_s (\mathbf{V}_s \cdot \nabla) \mathbf{v}_s' + \rho_s (\mathbf{v}_s' \cdot \nabla) \mathbf{V}_s$$

$$= -\nabla P_s - \nabla p_s' - A \rho_s \rho_n |\mathbf{V}|^2 \mathbf{V} - A \rho_s \rho_n |\mathbf{V}|^2 \mathbf{v}', \quad (39)$$

$$\rho_n \partial \mathbf{v}_n' / \partial t + \rho_n (\mathbf{V}_n \cdot \nabla) \mathbf{v}_n' + \rho_n (\mathbf{v}_n' \cdot \nabla) \mathbf{V}_n$$

$$+ \rho_s \partial \mathbf{v}_s' / \partial t + \rho_s (\mathbf{V}_s \cdot \nabla) \mathbf{v}_s' + \rho_s (\mathbf{v}_s' \cdot \nabla) \mathbf{V}_s$$

$$= \eta_n \nabla^2 \mathbf{V}_n + \eta_n \nabla^2 \mathbf{v}_n' - \nabla P - \nabla p'. \quad (40)$$

Since \mathbf{V}_n , \mathbf{V}_s , ∇P and ∇P_s are assumed to represent the laminar solutions, we have

$$0 = -\nabla P_s - A \rho_s \rho_n |\mathbf{V}|^2 \mathbf{V}, \quad (41)$$

$$0 = \eta_n \nabla^2 \mathbf{V}_n - \nabla P. \quad (42)$$

Thus Eqs. (39) and (40) reduce to

$$\rho_s \partial \mathbf{v}_s' / \partial t + \rho_s (\mathbf{V}_s \cdot \nabla) \mathbf{v}_s' + \rho_s (\mathbf{v}_s' \cdot \nabla) \mathbf{V}_s$$

$$= -\nabla p_s' - A \rho_s \rho_n |\mathbf{V}|^2 \mathbf{v}', \quad (43)$$

$$\rho_n \partial \mathbf{v}_n' / \partial t + \rho_n (\mathbf{V}_n \cdot \nabla) \mathbf{v}_n' + \rho_n (\mathbf{v}_n' \cdot \nabla) \mathbf{V}_n$$

$$+ \rho_s \partial \mathbf{v}_s' / \partial t + \rho_s (\mathbf{V}_s \cdot \nabla) \mathbf{v}_s' + \rho_s (\mathbf{v}_s' \cdot \nabla) \mathbf{V}_s$$

$$= \eta_n \nabla^2 \mathbf{v}_n' - \nabla p'. \quad (44)$$

Writing Eqs. (43) and (44) in terms of dimensionless variables ($t^* = t \bar{V}_s / d$, $\nabla^* = \nabla d$, $\mathbf{V}_s^* = \mathbf{V}_s / \bar{V}_s$, $\mathbf{v}_s^* = \mathbf{v}_s' / \bar{V}_s$, $\mathbf{V}_n^* = \mathbf{V}_n / \bar{V}_n$, $\mathbf{v}_n^* = \mathbf{v}_n' / \bar{V}_n$) gives

$$(\rho_n / \rho) [\partial \mathbf{v}_s^* / \partial t^* + (\mathbf{V}_s^* \cdot \nabla^*) \mathbf{v}_s^* + (\mathbf{v}_s^* \cdot \nabla^*) \mathbf{V}_s^*]$$

$$= -\nabla^* p_s^* / \rho - (A \rho d \bar{V}) |\mathbf{V}^*|^2 \mathbf{v}_s^*, \quad (45)$$

$$(\rho_n / \rho) [(\rho_n / \rho_s) \partial \mathbf{v}_n^* / \partial t^* + (\mathbf{V}_n^* \cdot \nabla^*) \mathbf{v}_n^* + (\mathbf{v}_n^* \cdot \nabla^*) \mathbf{V}_n^*]$$

$$+ (\rho_n / \rho) (\rho_n / \rho_s) [\partial \mathbf{v}_s^* / \partial t^*$$

$$+ (\mathbf{V}_s^* \cdot \nabla^*) \mathbf{v}_s^* + (\mathbf{v}_s^* \cdot \nabla^*) \mathbf{V}_s^*]$$

$$= -\nabla^* p^* / \rho + (1/R) \nabla^{*2} \mathbf{v}_n^*, \quad (46)$$

where

$$R = \rho \bar{V}_n d / \eta_n. \quad (47)$$

Equation (45) shows that one effect of the mutual friction is to couple the velocities \mathbf{v}_n^* and \mathbf{v}_s^* . The magnitude of the dimensionless number $\rho d A \bar{V}$ determines the importance of the mutual friction term, just as the Reynolds number R determines the importance of the viscous term in Eq. (46). The stability of the

normal fluid perturbation \mathbf{v}_n^* is determined by Eq. (46). This stability is dependent on the magnitude of R and the effect of the terms in \mathbf{v}_s^* . This latter effect is determined by the magnitude of $\rho d A \bar{V}$ in Eq. (45). We now postulate that the normal fluid perturbations become unstable at a particular value of $R = R_c$ determined by the value of $\rho d A \bar{V}$ and the system geometry. It is convenient to use the quantity

$$g = \rho d A \bar{V} / (1 + \rho d A \bar{V}) \quad (48)$$

which varies between zero and one, rather than $\rho d A \bar{V}$. Our assumption thus implies the existence of a universal function

$$R_c = R_c(g) \quad (49)$$

describing the onset of turbulence in the normal fluid. We might anticipate that for small coupling, R_c will have essentially its classical value, and decrease with increasing g . Our assumption is identical with the results of the Chandrasekhar and Donnelly calculation¹⁶ for flow between rotating cylinders. These authors find that the normal-fluid critical Taylor number T_c is a function of the coupling strength C [Eq. (28)]. Our assumption is, of course, highly speculative, but the results may provide an indication of qualitative behavior. We shall show that the existence of a function $R_c(g)$ offers an explanation for the observed temperature dependence of the critical Reynolds number in thermal counterflow, as well as critical-velocity effects found in several diverse experiments.

By using many different channels of different geometries, Chase² has demonstrated the relevance of the Reynolds number [Eq. (47)] in giving the temperature, channel size, and geometry dependence of W_c at low temperatures. He finds that as the temperature increases, the critical Reynolds number decreases. We can interpret this effect in terms of a decrease of R_c with g . Using Chase's results for $R_c(T)$ in cylindrical tubes, we have calculated a value of g for each (R_c, T) point. Plotting R_c against g then gives the result shown in Fig. 1. Figure 2 is a similar plot for his rectangular channel. The rapid drop in R_c at $g \approx 0.5$ is quite striking in both cases. Figure 3 shows similar calculations using the results of Brewer and Edwards¹⁹ in 366- μ and 107.6- μ diameter tubes.

The experiments of Staas, Taconis, and van Alphen³ can also be interpreted in terms of $R_c(g)$. In these measurements, critical Reynolds numbers were obtained from pressure-gradient measurements in a flow where $\mathbf{v} = \mathbf{v}_s - \mathbf{v}_n \approx 0$. From Eq. (48) then, we would expect g to be quite small, and thus R_c to have essentially its classical value (2300) independent of temperature. Indeed, it was found that $R_c = 1200$ for all temperatures and for three channel sizes. It would be

¹⁹ D. F. Brewer and D. O. Edwards, Phil. Mag. **7**, 721 (1962).

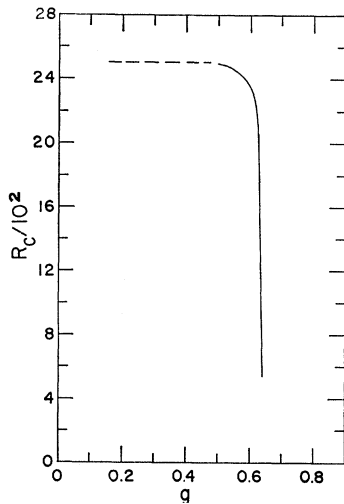


FIG. 1. The critical Reynolds number R_c as a function of the coupling parameter g [Eq. (48)], calculated from Chase's temperature gradient measurements in cylindrical channels. The dashed curve is an extrapolation to small values of g .

difficult to reconcile these results with those of Chase, for example, if R_c does not vary with the mutual friction.

Another measurement which can be interpreted in terms of a function $R_c(g)$ was reported by Chase.²⁰ In this experiment a rectangular channel (identical with that of Fig. 2) was rotated an angular frequency ω about either its long or short axes. The critical heat current was measured as a function of ω at 1.4°K. It was found that at low rotation speeds R_c was independent of ω but decreased rapidly with ω at higher values. In this case a large mutual friction is developed due to the rotation of the channel. The coupling constant g is thus no longer appropriate as it represents only the mutual friction due to the heat current W . In Fig. 4 we show Chase's R_c data plotted against the rotation coupling constant of Chandrasekhar and Donnelly [Eq. (28)]. Comparison of Figs. 2 and 4 reveals a striking similarity. This experiment is the converse of that of Staas *et al.*³ In the latter case the mutual friction was reduced from the equivalent-heat-

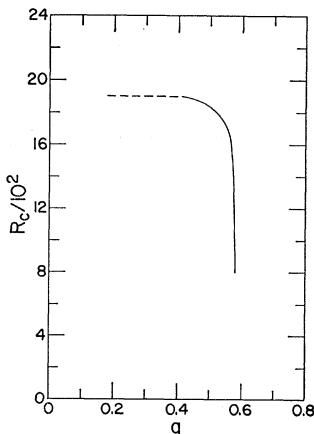


FIG. 2. The critical Reynolds number R_c as a function of the coupling parameter g [Eq. (48)] calculated from Chase's temperature gradient measurements in a rectangular channel. The dashed curve is an extrapolation to low g values.

²⁰ C. E. Chase, in *Proceedings of the VIIth Conference on Low Temperature Physics* (University of Toronto Press, Toronto, 1961), p. 438.

current flow and the critical Reynolds number remained constant. In the former case the mutual friction was increased from the heat current value and R_c was reduced.

Without a detailed calculation of the function $R_c(g)$ it is only possible to give a qualitative description of the critical heat current W_c . In general, the critical Reynolds number will increase with decreasing temperature reaching its classical value at about 1.3°K. The classical value is a function of geometry only ($R_c \approx 2300$ for circular tubes, ≈ 1400 for rectangular channels) but may be expected to vary somewhat from these values because of length effects, entrance shape, and roughness. This general behavior of R_c results in a temperature variation of W_c as shown in Fig. 5. This temperature variation is in qualitative agreement with all available critical-heat-current data.

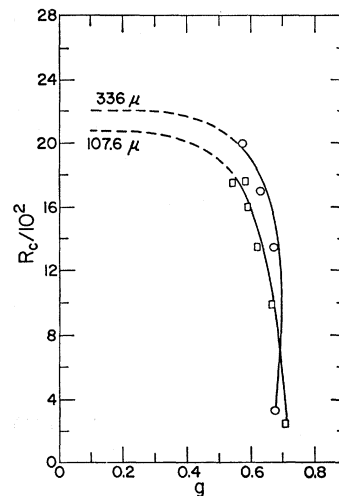


FIG. 3. The critical Reynolds number R_c as a function of the coupling parameter g [Eq. (48)] calculated from Brewer and Edwards temperature-gradient measurements in 366- μ and 107.6- μ diameter channels (circles and squares, respectively). The dashed curves are extrapolations to low g values.

The critical heat current W_0 is assumed to result from superfluid turbulence originating at v_{s0} . With v_{s0} given by the Feynman formula [Eq. (11)], we then have

$$W_0 = (\hbar/md) \ln(d/2a_0) \rho S T (\rho_s/\rho_n). \quad (50)$$

The temperature dependence of W_0 is shown qualitatively in Fig. 5. Experimentally it is found that $v_{s0}d$ is not independent of temperature as given in Eq. (11). Some investigators find it to be an increasing function of T ,²¹ others to be a decreasing function of T ,²² and others find $v_{s0}d$ increases at low T and decreases at high T .²³ Recent experiments by Allen *et al.*⁵ suggest that W_0 may depend markedly on geometrical irregularities in the channel or heater. In all cases, however, the magnitude of the temperature variation is small enough so that the qualitative behavior shown in Fig. 5 is not significantly altered.

²¹ D. F. Brewer and D. O. Edwards, *Phil. Mag.* **6**, 775 (1961).

²² J. N. Kidder and W. M. Fairbank, *Phys. Rev.* **127**, 987 (1962).

²³ F. A. Staas and K. W. Taconis, *Physica* **27**, 924 (1961).

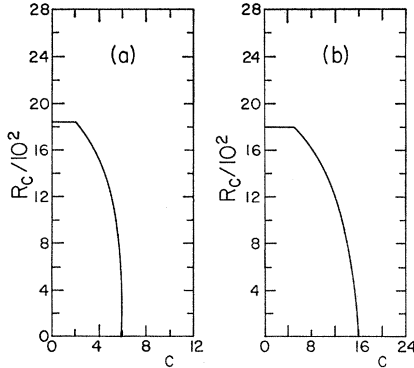


FIG. 4. The critical Reynolds number R_c as a function of the rotational coupling parameter C [Eq. (28)] calculated from Chase's temperature-gradient measurements in a rotating rectangular channel. Results are shown for rotation about an axis parallel to the long side (a) and short side (b) of the rectangular channel.

III. THE EFFECTS OF TURBULENCE

The assumption that there are two critical heat currents W_0 and $W_c > W_0$ defines three regions of interest. The first, $W < W_0$, is the subcritical regime and was treated in Sec. I. In the second region, $W_0 < W < W_c$, the superfluid is turbulent. This turbulence is probably in the form of a "tangled mass of vortex line" as described by Vinen,¹ and generates the mutual friction force. In the third region, $W > W_c$, both the normal and superfluid are turbulent. In the second and third regions the hydrodynamic behavior of the normal fluid is scaled by the Reynolds number in Eq. (47). That is, it behaves as if it had a density ρ rather than ρ_n due to its coupling to the superfluid. We shall treat the normal fluid as a classical turbulent fluid in the third region. Support for this assumption comes from the Chandrasekhar and Donnelly calculation¹⁶ which shows that the normal-fluid instability in rotation is of the classical Taylor type. Direct evidence for three distinct flow regions essentially as described above has recently been obtained by Allen, Griffiths and Osborne.⁵ We shall defer discussion of this experiment to the latter part of Sec. IV.

In terms of these assumptions, any nonlinear effects occurring in the second region are a result of superfluid turbulence. Vinen,²⁴ as well as others,²⁵⁻²⁷ has suggested that the presence of vortex lines in the superfluid could give rise to a superfluid eddy viscosity η_s . This would result in a superfluid force

$$F_s = \eta_s \nabla^2 v_s; \quad v_s > v_{s0} \quad (51)$$

²⁴ W. F. Vinen, *Progress in Low Temperature Physics*, edited by C. J. Gorter (North-Holland Publishing Company, Amsterdam, 1960), Vol. III, Chap. 1.

²⁵ K. R. Atkins, *Liquid Helium* (Cambridge University Press, London, 1959).

²⁶ D. F. Brewer and D. O. Edwards, *Phil. Mag.* **6**, 1173 (1961).

²⁷ P. P. Craig, in *Proceedings of the VIIIth International Conference on Low Temperature Physics* (Butterworths Scientific Publications Ltd., London, 1963), p. 102.

to be added to the right-hand side of Eq. 2. The "pure superflow" experiments of Kidder and Fairbank²² have been interpreted in terms of such a force. Using an elaborate and sensitive pressure-measuring technique, they find that above a critical superfluid velocity v_{s0} , a pressure gradient

$$\nabla P = \alpha(v - v_0)v = F_s \quad (52)$$

is observed. Their measurements were confined to one tube diameter ($d = 1.1$ mm) and to four temperatures ($T = 1.26, 1.30, 1.48, 1.57^\circ\text{K}$). The quantity α was found to vary slowly with temperature, and was approximately 0.2 cgs units. Recent isothermal-flow measurements by Kidder and Blackstead²⁸ at 0.4°K give similar results for a wide range of diameters. Although in neither of these cases are the boundary conditions expected to be identical with those in thermal counterflow, the results strongly suggest a force of the type given in Eq. (52) may be present. Taken together, Eqs. (51) and (52) imply that η_s should depend simply on the mean spacing of vortex lines. If such an interpretation is correct, a superfluid eddy viscosity should also be observed in rotation experiments where, for rotation at angular frequency ω , the mean spacing of vortex lines is proportional to $\omega^{1/2}$.¹⁴ Indeed, Craig²⁷ has shown that the velocity profiles measured in a rotating-bucket experiment are most simply interpreted in terms of an eddy viscosity proportional to $\omega^{1/2}$. For consistency, the normal fluid Reynolds number in Eq. (49) should be defined with a total viscosity $\eta_n + \eta_s$. Experimentally, however, $\eta_n \gg \eta_s$ so that the qualitative results of Sec. II are not significantly affected.

In the second region, the flow of the normal fluid is laminar, and the pressure gradient necessary to produce a mean velocity $\langle v_n \rangle$ in a circular tube of radius a is found

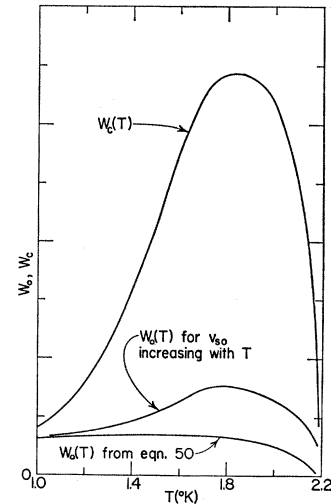


FIG. 5. The qualitative temperature dependence of the critical heat currents W_0 and W_c . W_0 and W_c are plotted on the same arbitrary vertical scale.

²⁸ J. N. Kidder and H. A. Blackstead, in *Proceedings of the IXth International Conference on Low Temperature Physics* (Plenum Press, Inc., New York, 1965), p. 331.

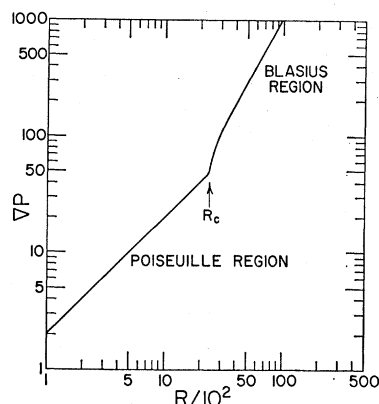


FIG. 6. The qualitative dependence of pressure gradient on Reynolds number for a classical fluid. The pressure gradient is plotted on an arbitrary scale.

by solving Eq. (42).

$$\nabla P = -8\eta_n \langle v_n \rangle / a^2 = \nabla P_0. \quad (53)$$

Since this expression does not involve the density, the normal fluid pressure gradient in the second region is identical with that in the subcritical region [Eq. (6)]. In the third region ($W > W_c$) the normal fluid is turbulent and the pressure gradient is no longer a linear function of $\langle v_n \rangle$. A classical fluid described by the quantities ρ , v_n and η_n flowing in a tube of diameter d has three distinct flow regimes. For $R < R_c$, the flow is laminar and the pressure gradient is that given by Eq. (53). For $R \gtrsim 2R_c$, the flow is in a fully developed turbulent state and may be treated by statistical

methods. In this case the pressure gradient is given by an empirical expression due to Blasius.²⁹

$$\nabla P = (0.133/R^{1/4})\rho \langle v_n \rangle^2 / d. \quad (54)$$

This expression can also be obtained from semiempirical theories of turbulent flow such as Prandtl's mixing length theory.²⁹ As in Eq. (52) for the superfluid, we can interpret this pressure gradient as an effective normal-fluid body force.

$$F_n = (0.133/R^{1/4})(\rho \langle v_n \rangle^2 / d); \quad R \gtrsim 2R_c. \quad (55)$$

In the regime of Reynolds numbers $R_c < R < 2R_c$, the flow is in a state of transition from laminar to turbulent flow. Pressure gradients in this region tend to show large fluctuations in time and are greater than the laminar value [Eq. (53)] but less than the turbulent value [Eq. (54)].³⁰ This behavior is shown qualitatively in Fig. 6. In terms of the usual hydrodynamic stability analysis⁶ (Sec. II), this region is understood in terms of the growth of unstable perturbations on the laminar flow. Landau⁶ has shown on quite general grounds that the magnitude of these velocity perturbations increases with R as

$$v' = \text{const}(R - R_c)^{1/2} \quad (56)$$

for R close to R_c . Recent experiments by Donnelly³¹ and Donnelly and Schwarz³² have directly verified this "Landau law" in the case of Couette flow. When R becomes substantially greater than R_c , these perturbations occur over a wide range of frequencies and the flow is fully turbulent.

The pressure gradient in the transition region may be accounted for, at least approximately, in terms of an

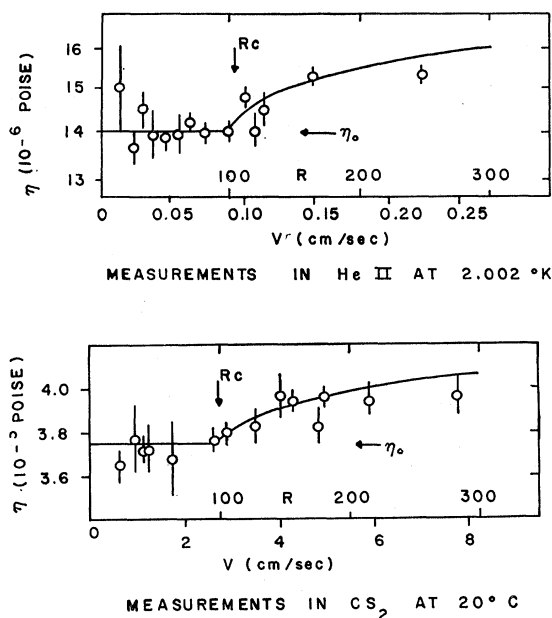


FIG. 7. The effective viscosity of CS_2 and He II measured in a rotating cylinder viscometer as a function of the cylinder velocity and corresponding Reynolds number. The open circles are the data of Woods and Hollis-Hallett. The solid lines are plots of $\eta = \eta_0 + \eta_{ne}$ with η_{ne} given by Eq. (57) using $\beta = 0.17 \mu\text{P}$ for He II and $\beta = 0.025 \text{ mP}$ for CS_2 .

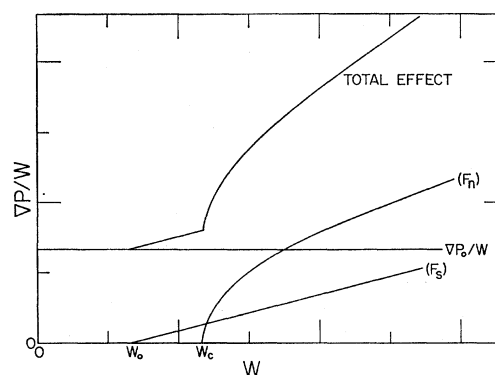


FIG. 8. The qualitative dependence of $\nabla P/W$ on heat current. The total effect is shown as the sum of contributions from normal fluid turbulence (F_n) and superfluid turbulence (F_s). The $\nabla P/W$ scale is arbitrary.

²⁹ L. Prandtl, *Essentials of Fluid Dynamics* (Hafner Publishing Company, New York, 1952).

³⁰ R. R. Rothfus, C. C. Monrad, and V. E. Senecal, *Ind. Eng. Chem.* **42**, 2511 (1950).

³¹ R. J. Donnelly, *Phys. Rev. Letters* **10**, 282 (1963).

³² R. J. Donnelly and K. W. Schwarz, *Phys. Letters* **5**, 322 (1963).

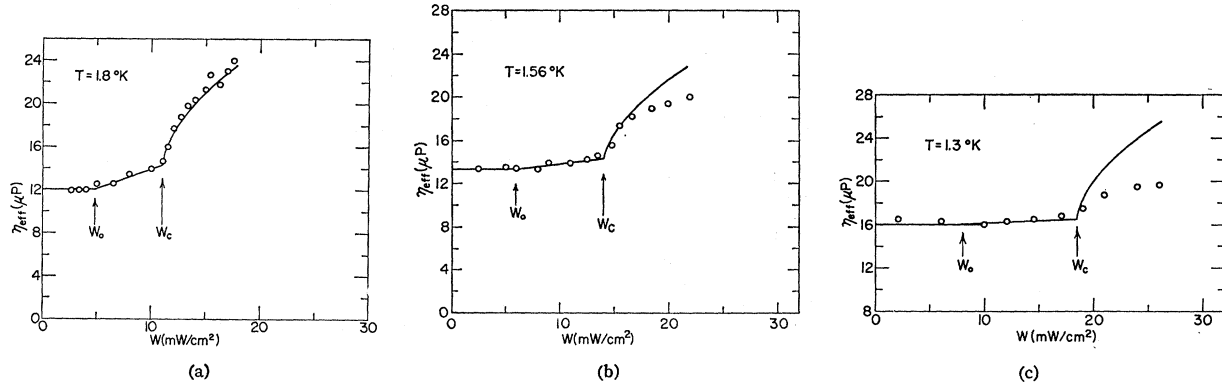


FIG. 9. The effective normal fluid viscosity η_{eff} obtained from $\nabla P/W$ for a 107.6- μ diameter channel. The open circles are the measured values of Brewer and Edwards, and the solid lines the effective viscosity calculated from equations given in the text. Results are for 1.3, 1.56, and 1.8°K.

eddy viscosity due to the perturbations [Eq. (56)] of the form

$$\eta_{ne} = \beta(R - R_c)^{1/2}, \quad (57)$$

where β may be expected to vary with system geometry and temperature. Evidence for this eddy viscosity can be adduced from the rotating cylinder measurements of Woods and Hollis-Hallett.³³ In these experiments the outer cylinder was rotated and the viscosity of the working fluid obtained from the torque on the inner. Measurements were made on CS₂ and He II, and the results are shown in Fig. 7. The results are consistent with an eddy viscosity of the form given in Eq. (57) and clearly show the similarity of He II flow to classical flow. Note in particular that the critical Reynolds number for the He II and CS₂ are identical within experimental error.

The vibrating-wire measurements of Tough, McCormick and Dash⁴ also can be interpreted in terms of a normal-fluid eddy viscosity. In these experiments the damping force on a fine wire in He II was measured as a function of heat current. Below the critical heat current W_c the damping was due solely to the normal fluid viscosity, η_n . Above W_c an excess damping force was observed which varied as $(R - R_c)^{1/2}$. This can be interpreted as the effect of a normal fluid eddy viscosity as in Eq. (57).

For lack of a more detailed theory of the transition region, therefore, we will assume that the pressure gradient is given by the laminar expression [Eq. (53)] with an effective viscosity $\eta_n + \eta_{ne}$:

$$\begin{aligned} \nabla P &= -(8/a^2)(\eta_n + \eta_{ne})\langle v_n \rangle \\ &= \nabla P_0 + F_n; \quad R_c < R < 2R_c. \end{aligned} \quad (58)$$

The eddy viscosity is given by Eq. (57) with β an undetermined parameter. We shall fix β by requiring that F_n given by Eqs. (57) and (58) join smoothly to F_n

given by Eq. (55) at $2R_c$ as in Fig. 6. Such an approach cannot be expected to give great accuracy, but might yield agreement with experiment.

IV. TEMPERATURE AND PRESSURE GRADIENTS IN THERMAL COUNTERFLOW

Using F_s , F_n and F_{sn} developed in the previous sections, the pressure and temperature gradients can be written

$$\nabla P = \eta_n \nabla^2 v_n - F_s - F_n, \quad (59)$$

$$\rho_s S \nabla T = (\rho_s/\rho) \nabla P + F_{sn} + F_s. \quad (60)$$

Defining the subcritical values (Sec. I):

$$\nabla P_0 = \eta_n \nabla^2 v_n, \quad (61)$$

$$\rho_s S \nabla T_0 = \nabla P_0, \quad (62)$$

we have

$$\nabla P = \nabla P_0 - F_s - F_n \quad (63)$$

$$\nabla T = \nabla T_0 + (\rho_n/\rho) F_s/\rho S - F_n/\rho S + F_{sn}/\rho_s S. \quad (64)$$

The qualitative dependence of $\nabla P/W$ on W given by Eq. (63) with F_s and F_n given by Eqs. (52), (55) and (58) is shown in Fig. 8. There is a linear increase in $\nabla P/W$ for $W > W_0$ due to F_s , followed by a relatively abrupt increase at W_c . For $W \gg W_c$, $\nabla P/W$ should vary as W or $W^{3/4}$ depending on whether F_s or F_n is the larger. The relative magnitudes of the F_s and F_n contributions will depend on the dimensions of the system and temperature. The behavior shown in Fig. 8, however, is qualitatively like that found in all pressure-gradient measurements.

Let us consider in detail the pressure gradient measurements of Brewer and Edwards.²⁶ They used a 107.6- μ diameter conduction tube and measured the pressure gradient as a function of heat current for temperatures of 1.8, 1.56 and 1.3°K. The present their data in the form of an effective viscosity defined as

$$\eta_{\text{eff}} = (a^2 \rho_s S T / 8) \nabla P / W \quad (65)$$

³³ A. D. B. Woods and A. C. Hollis-Hallett, *Proceedings of the Vth International Conference on Low Temperature Physics & Chemistry* (University of Wisconsin Press, Madison, Wisconsin, 1958), p. 16.

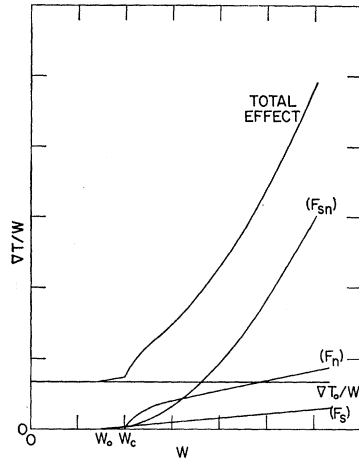


FIG. 10 The qualitative dependence of $\nabla T/W$ on heat current. The total effect is shown as the sum of contributions from normal fluid turbulence (F_n), superfluid turbulence (F_s), and mutual friction (F_{sn}). The $\nabla T/W$ scale is arbitrary.

as a function of the relative velocity

$$v = W/\rho_s ST. \quad (66)$$

Using F_s given in Eq. (52) and F_n given by Eqs. (55) and (58), we have calculated η_{eff} . The calculations are shown as solid lines in Fig. 9 along with Brewer and Edwards' measurements. A value of α [Eq. (52)] of 0.2 cgs units was found to fit all the data. There seems to be a systematic discrepancy which is largest at 1.3°K. This may, however, be a result of the approximate treatment of the transition region. Staas *et al.*³ have made pressure-gradient measurements at 1.7°K in a 255 μ tube up to $\approx 3W_c$. They find that the pressure gradient above W_c is equal to that given by Blasius' expression [Eq. (54)] which we have called F_n . This result is somewhat surprising in that for a 255- μ tube at 1.7°K we calculate a value of F_s essentially equal to F_n , if α is taken to be 0.2. This would result in $\nabla P/W$ varying essentially as W , but with about twice the magnitude given by F_n alone.

In a series of measurements made over a wide temperature range with 82- μ , 174- μ and 255- μ tubes, and with a flow designed to give $v_s \approx v_n$, Staas *et al.*³ find that again Blasius' pressure-gradient expression [Eq. (54)] agrees with experiment. In this case, however, F_s is approximately zero since $v = v_s - v_n \approx 0$, and we would expect only F_n to contribute to the pressure gradient, in agreement with experiment.

The values of the critical heat currents W_0 and W_c corresponding to v_{s0} and v_{nc} , which were considered quantitatively in Sec. II, are shown in Fig. 9. There is little difficulty in locating W_c from pressure-gradient measurements. W_0 becomes difficult to measure in small channels at low temperatures when F_s becomes quite small. Fortunately W_0 is readily measured in temperature gradient measurements.

The qualitative behavior of $\nabla T/W$, the thermal resistance as given by Eq. (64), is shown in Fig. 10. Here we expect the F_{sn} term to dominate at high heat currents since it increases most rapidly with W . As

mentioned in Sec. II, we have neglected any "build-up" process in the mutual friction which might modify F_{sn} at low ($W \approx W_0$) heat currents. Vinen's measurements of transient effects¹ clearly demonstrate that such a "build-up" process does exist, however. The temperature gradient measurements of Brewer and Edwards²¹ made in a 52- μ tube at low ($W \approx W_0$) heat currents clearly show the effect of this "build-up" on the thermal resistance to be confined to a small "transition region" near W_0 . They also noted large spontaneous fluctuations in the temperature gradient in this region. Referring again to Fig. 10, it can be seen that the "bump" in the thermal resistance is due to the onset of the F_n term at W_c . Unlike the pressure-gradient results, if $W_c \gg W_0$ the effect of F_n on the total resistance becomes negligible.

We consider in detail the temperature-gradient measurements of Chase² made in 0.080-cm diameter tubes. Chase presents his data in terms of an excess temperature gradient:

$$\nabla T^* = \nabla T - \nabla T_0, \quad (67)$$

where ∇T_0 is given by Eq. (62) and ∇T is the measured gradient. We have calculated ∇T^* from Eq. (64) at 1.15, 1.3 and 1.8°K using F_s , F_{sn} , and F_n given by Eqs. (52), (15), (55), and (58). Since A , the mutual friction constant, is found to vary from one system to another,¹⁵ we have treated it as a parameter, choosing A such that the calculated and experimental temperature gradients agree at the highest measured heat current. In this region F_{sn} is the dominant contribution to the thermal resistance and it is felt this fitting procedure is justified. The resulting values of A agree closely with those found by Kramers¹⁵ in a 2.6-mm diameter tube.

In Fig. 11 we show the calculated ∇T^* along with some of Chase's data. At all three temperatures the

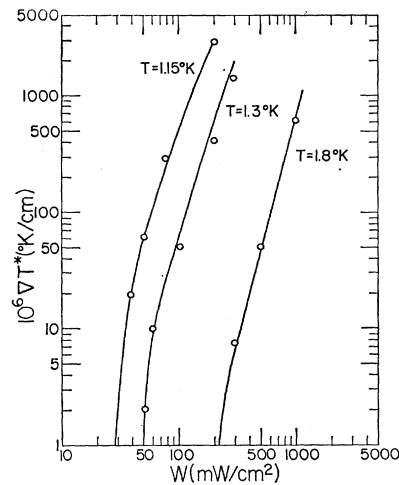


FIG. 11. The excess temperature gradient ∇T^* [Eq. (67)] for an 0.08-cm diameter channel. The open circles are the measured values of Chase, and the solid lines the excess temperature gradient calculated from equations given in the text. Results are for 1.15, 1.3, and 1.8°K.

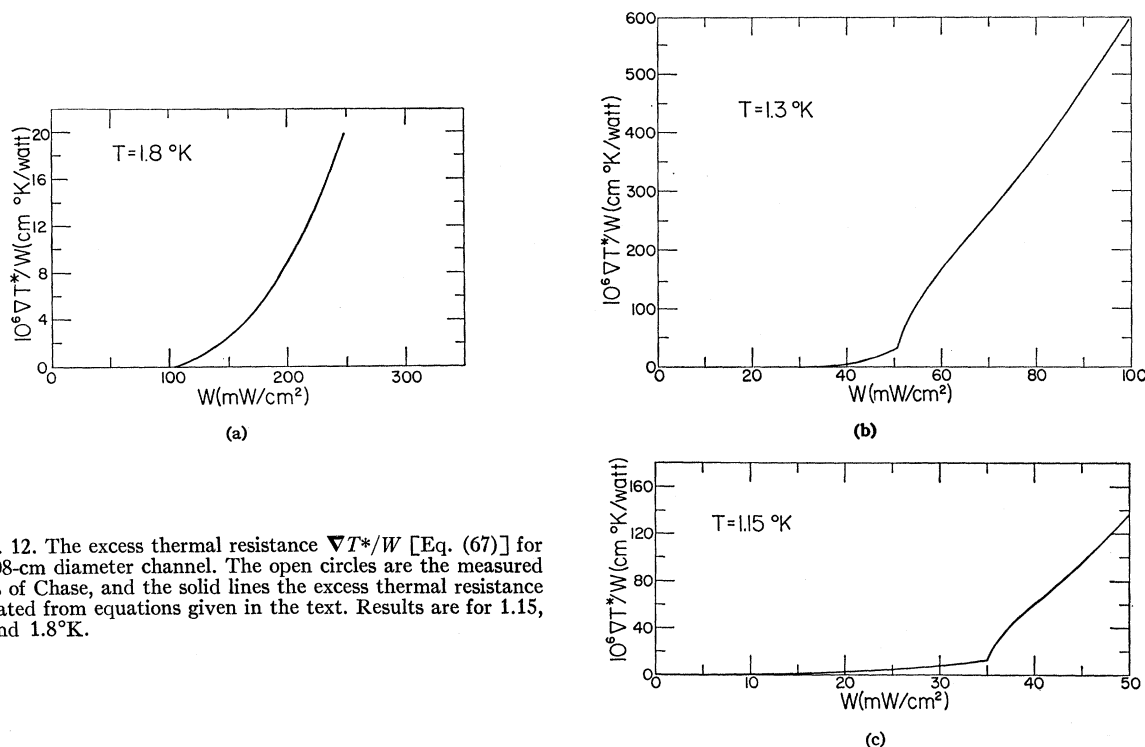


FIG. 12. The excess thermal resistance $\nabla T^*/W$ [Eq. (67)] for an 0.08-cm diameter channel. The open circles are the measured values of Chase, and the solid lines the excess thermal resistance calculated from equations given in the text. Results are for 1.15, 1.3, and 1.8°K.

agreement is quite good. Note in particular the marked curvature of the 1.15°K curve due to a large contribution from F_n . In Fig. 12 we show the excess thermal resistance $\nabla T^*/W$ for low heat currents. At the low temperatures 1.15 and 1.3°K, the “bump” due to the onset of F_n at W_c is quite dominant, but at 1.8°K has become masked by the F_{sn} term. This effect has also been observed by Vinen¹ and others. It is difficult to explain this phenomenon without the assumption of two critical heat currents. Vinen²⁴ refers to W_c as the critical heat current and regards the rise in thermal resistance for $W < W_c$ as due to “subcritical turbulence.” Brewer and Edwards,¹⁹ on the other hand, regard W_0 as the critical heat current and interpret the rise in resistance at W_c as due to a mutual friction build-up process. This interpretation of thermal resistance can also be applied to temperature gradients measured in “pure superflow.” In that case the thermal resistance is found to increase smoothly with no evidence of a “bump.”³⁴ This is consistent with the present model, since the “bump” is thought to arise from the onset of normal-fluid turbulence which is absent in these experiments.

The velocity-field measurements of Allen, Griffiths and Osborne⁵ to a large extent offer direct experimental verification for the nature of the three flow regions.

³⁴ T. M. Wiarda, G. von den Heyden, and H. C. Kramers, *Proceedings of the IXth International Conference on Low Temperature Physics* (Plenum Press, Inc., New York, 1965), p. 284.

Using a fine quartz fiber to detect circulation and velocity fluctuations in a heat current, they have demonstrated the existence of three distinct flow regions. In the first (subcritical) region they find that the normal fluid is laminar and the superfluid undisturbed. Observations in the second region suggest an increasing density of disordered vortex line in the superfluid. The third region is characterized by random fluctuations of the normal-fluid velocity as would be expected in turbulent flow.

In general, then, it appears that the present model based on normal and superfluid turbulence gives a qualitative and often quantitative description of temperature and pressure gradients in thermal counterflow, as well as critical heat currents. It also provides a framework in which such diverse experiments as “pure superflow”^{21,27} and the Staas, Taconis, van Alphen experiment ($\mathbf{v}_n - \mathbf{v}_s \approx 0$) may be understood. While there is every reason to believe that He II flow phenomena are far more complicated than presented here, it is felt that the present model offers a new and promising basis for future study.

ACKNOWLEDGMENTS

The author wishes to thank the National Science Foundation for their generous support, as well as J. G. Dash and D. O. Edwards for several informative discussions of the problem.